Improvement in performance of hydrogenated amorphous silicon cells with hydrogenated intrinsic amorphous silicon oxide p/i buffer layers

Jia Fang, Ze Chen, Ning Wang, Lisha Bai, Guofu Hou *, Xinliang Chen, Changchun Wei, Guangcai Wang, Jian Sun, Ying Zhao, Xiaodan Zhang *

Institute of Photo-Electronics Thin Film Devices and Technology of Nankai University, Key Laboratory of Photo-electronic Thin Film Devices and Technology, Tianjin 300071, PR China

ABSTRACT

In the study, we inserted different types of intrinsic and p-type layers as the p/i buffer layer in hydrogenated amorphous silicon (a-Si:H) solar cells and investigated their effects on device performance. The band gap and activation energy of the buffer layer had a significant effect on the open-circuit voltage (V_{oc}) of the cells. Inserting a hydrogenated intrinsic amorphous silicon oxide (i-a-SiO$_x$:H) layer as the p/i buffer layer in a-Si:H solar cells leads to a significant V_{oc} increase up to 909 mV. It also increased the external quantum efficiency at 400 nm to 75%. This was primarily owing to the increase in the built-in electric field and a decrease in the rate of carrier recombination at the p/i interface. Finally, the initial conversion efficiencies of single-junction a-Si:H solar cell and hydrogenated amorphous silicon/hydrogenated microcrystalline silicon (a-Si:H/μc-Si:H) tandem solar cell could be increased to 10.64% and 12.24%, respectively.

© 2014 Elsevier B.V. All rights reserved.

1. Introduction

Silicon oxide materials are being investigated for use in thin-film silicon solar cells because they exhibit low absorption and low refractive index, owing to the incorporated oxygen [1–3]. Films of p-type hydrogenated microcrystalline silicon oxide (p-μc-SiO$_x$:H) have a diphasic structure, in which microcrystalline silicon filaments are surrounded by an oxygen-rich amorphous silicon oxide phase [4,5]. These films, which exhibit several desirable characteristics, have been studied extensively in order to improve the performance of solar cells [6–8]. Firstly, owing to the shunt-quenching effect [9,10], p-μc-SiO$_x$:H films can improve the open-circuit voltage (V_{oc}) and fill factor (FF) of solar cells even when fabricated on highly textured substrates. Secondly, p-μc-SiO$_x$:H films can also serve as an antireflective layer to reduce the reflection of incident sunlight, given their low refractive index [10,11]. Lastly, p-μc-SiO$_x$:H films can also be used as a contact layer, as their electrical and optical properties can be readily tuned [12]. However, the band gap (E_{04}) of p-μc-SiO$_x$:H window layers, which ranges from 2.0 eV to 2.6 eV [3,7,8], is higher than that

of hydrogenated intrinsic amorphous silicon (i-a-Si:H) layers. This can result in a band gap mismatch and an increase in the rate of recombination of carriers at the p/i interface, leading to deterioration in the overall device performance. Thus, a thin buffer layer should be inserted at the p/i interface to prevent this problem [13–15].

Different types of buffer layers have been introduced at the p/i interface to improve the performance of photovoltaic devices [13–15]. In the case of n–i–p cells, the p-μc-SiO$_x$:H layer can be deposited directly on the i-a-Si:H layer. Because the p-μc-SiO$_x$:H layer is grown by an epitaxy-like process, an amorphous incubation layer is formed at the p/i interface during the initial deposition stage [13]. This naturally forming amorphous incubation layer functions as a p/i buffer layer and reduces the carrier recombination rate at the p/i interface, in addition to increasing V_{oc} [14]. On the other hand, in p–i–n solar cells, an extra p/i buffer layer needs to be inserted at the interface. Since the i-a-SiO$_x$:H film has a wide band gap range from 1.76 eV to 2.43 eV [16], it can be used as a p/i buffer layer. Bugnon et al. [15] were able to insert an i-a-SiO$_x$:H p/i buffer layer successfully and found that the layer could prevent boron cross contamination. As a result, the initial- and degraded-state performances were both improved significantly. However, further studies on the effects of i-a-SiO$_x$:H p/i buffer layers on device performance are necessary.

In this study, to understand the role of i-a-SiO$_x$:H buffer layers in a-Si:H solar cells, four different types of p/i buffer layers, namely, i-a-SiO$_x$:H, i-a-Si:H, p-type hydrogenated amorphous silicon oxide (p-a-SiO$_x$:H), and p-type hydrogenated amorphous silicon (p-a-Si:H) layers, were prepared and characterised. We focused on the band gaps and activation energies (E_a) of the layers. An initial efficiency as high as 10.64% was achieved in the case of a single-junction a-Si:H solar cell with an i-a-SiO$_x$:H layer as the p/i buffer layer.

2. Materials and methods

2.1. Fabrication of the different buffer layers

The different buffer layers were deposited at a temperature of 210 °C using a radio frequency plasma-enhanced chemical vapour deposition (RF-PECVD) cluster system. The intrinsic Si layer was deposited using a mixture of hydrogen and silane. The p-type Si film and the SiO$_x$ films were obtained by adding trimethylboron and carbon dioxide (CO$_2$), respectively, to the mixture.

Films with a thickness of 20 nm were deposited on glass substrates (Eagle 2000, Corning) in order to investigate the properties of the different layers. The activation energy of the films was estimated from their temperature-dependent dark conductivity, σ_d, using the following equation:

$$\sigma d(T) = \sigma 0 \exp(-Ea/kT), \tag{1}$$

where σ_0 is the conductivity pre-factor, k is the Boltzmann constant, and T is the absolute temperature. The Tauc optical gap (E_g) values were obtained from the optical reflection and transmission spectra.
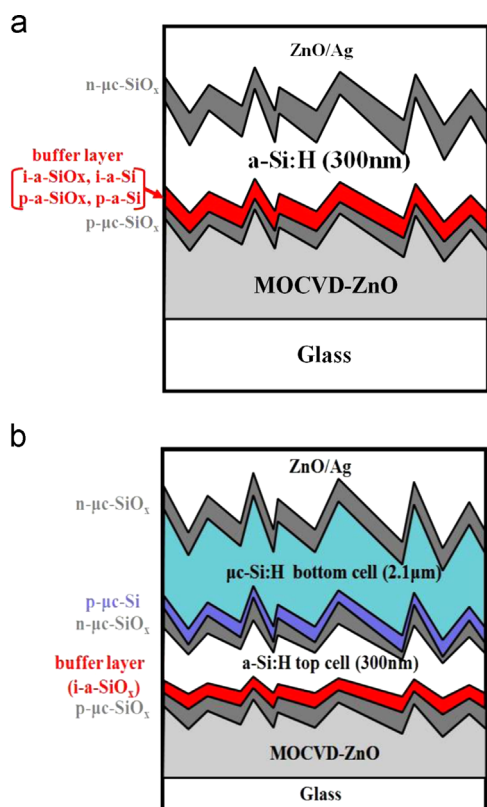

Fig. 1. Schematic diagrams of p–i–n solar cells: (a) single-junction a-Si:H cell with different p/i buffer layers and (b) a-Si:H/μc-Si:H tandem cell with i-a-SiO$_x$:H buffer layer in the top cell.

2.2. Fabrication of p–i–n solar cells

The p–i–n a-Si:H and a-Si:H/μc-Si:H tandem solar cells were deposited on textured zinc oxide (ZnO) at a substrate temperature of 210 °C. Fig. 1 (a) and (b) shows the respective device structures of the cells. The active area of the cells was 0.253 cm^2. The thickness of the intrinsic layer was 300 nm for the single-junction a-Si:H cell and top cell in the tandem cell. The thickness of the intrinsic layer of the bottom cell was 2.1 μm. Front electrodes were grown by metalorganic chemical vapour deposition (MOCVD). The root mean square roughness of the ZnO layer was 90 nm. The surface of the ZnO layer consisted of randomly distributed pyramidal structures [17]. The current–voltage (J–V) characteristics of the cells were measured in the dark and under light using a dual-lamp solar simulator (WXS-156S-L2, AM1.5GMM). The tests were performed under standard conditions (AM1.5, 100 mW/cm^2) at 25 °C. The spectral responses of the cells were obtained from external quantum efficiency (EQE) measurements (QEX10, PV Measurement), and the short-circuit current densities (J_{sc}) were calculated from the EQE values.

3. Results and discussion

3.1. Optoelectronic characteristics of the different buffer layers

The p/i buffer layer should have a band gap that lies between the band gaps of the p-type window layer and the intrinsic absorption layer. The position of the Fermi level of the p/i interface has an effect on the performance of the cell [18,19]. Therefore, E_g and E_a are critical parameters for improving cell performance. As mentioned previously, four different buffer layers were fabricated by optimising the deposition conditions. Table 1 lists the deposition parameters, the values of E_g and E_a of the different buffer layers.

The E_g value of sample A (i-a-SiO$_x$:H) was 1.86 eV and slightly higher than that of the i-a-Si:H layer (1.75–1.85 eV). This means the oxygen content of sample A was low. The E_a value of sample A (0.51 eV) was less than $E_g/2$ (=0.93 eV), which indicates that the Fermi level of this film was lower than the mid-gap level during the initial phase of the oxygen incorporation process. That is to say, the electrical properties of sample A were similar to those of lightly doped p-type SiO$_x$ films. Because the oxygen content of i-a-SiO$_x$:H films determines their E_a values [20], if $E_a > E_g/2$ for films with high E_g values, it means that the films have high oxygen contents. When the CO$_2$ flow was increased to 5 sccm (data not shown), the E_g and E_a values became 2.01 eV and 1.02 eV, respectively.

Hydrogen dilution in sample B (i-a-Si:H) ensured that the film remained in the amorphous phase. Thus, the E_g and E_a values of the film were 1.82 eV and 0.9 eV, respectively.

The higher hydrogen dilution in sample C (p-a-SiO$_x$:H) was beneficial to oxygen incorporation [21]. Thus, E_g of sample C was similar to sample A, which was prepared at a lower CO$_2$ flow. Further, even though the higher hydrogen dilution of sample C

Table 1
Deposition parameters, the values of the E_g and E_a of the different buffer layers.

Sample	Buffer type	SiH$_4$ (sccm)	H$_2$ (sccm)	B(CH$_3$)$_3$ (sccm)	CO$_2$ (sccm)	E_g (eV)	E_a (eV)
A	i-a-SiO$_x$:H	6	170	–	2	1.86	0.51
B	i-a-Si:H	10	200	–	–	1.82	0.9
C	p-a-SiO$_x$:H	3	400	2	0.5	1.84	0.35
D	p-a-Si:H	3	200	2	–	1.78	0.33